# Cantilever Array Sensors Detect Specific Carbohydrate–Protein Interactions with Picomolar Sensitivity

**Kathrin Gruber,[†,‡] Tim Horlacher,[§] Riccardo Castelli,[§] Andreas Mader,[†] Peter H. Seeberger,[§,∥,*] and Bianca A. Hermann[‡,*]**

[†]Department of Physics, Ludwig-Maximilians-Universität Munich, Walther-Meissner-Strasse 8, 85748 Garching, Germany, [‡]Walther-Meissner-Institute & CeNS, Walther-Meissner-Strasse 8, 85748 Garching, Germany, [§]Department of Biomolecular Systems, Max Planck Institute of Colloids and Interfaces, Arnimallee 22, 14195 Berlin, Germany, and [∥]Institute for Chemistry and Biochemistry, Freie Universität Berlin, Arnimallee 22, 14195 Berlin, Germany

**ABSTRACT** Advances in carbohydrate sequencing technologies have revealed the tremendous complexity of the glycome. This complexity reflects the structural and chemical diversity of carbohydrates and is greater than that of proteins and oligonucleotides. The next step in understanding the biological function of carbohydrates requires the identification and quantification of carbohydrate interactions with other biomolecules, in particular, with proteins. To this end, we have developed a cantilever array biosensor with a self-assembling carbohydrate-based sensing layer that selectively and sensitively detects carbohydrate–protein binding interactions. Specifically, we examined binding of mannosides and the protein cyanovirin-N, which binds and blocks the human immunodeficiency virus (HIV). Cyanovirin-N binding to immobilized oligomannosides on the cantilever resulted in mechanical surface stress that is transduced into a mechanical force and cantilever bending. The degree and duration of cantilever deflection correlates with the interaction's strength, and comparative binding experiments reveal molecular binding preferences. This study establishes that carbohydrate-based cantilever biosensors are a robust, label-free, and scalable means to analyze carbohydrate–protein interactions and to detect picomolar concentrations of carbohydrate-binding proteins.

**KEYWORDS:** cantilever array sensors · glycomics · nanomechanics · biosensors · cyanovirin-N

Recent advances in technologies for sequencing and synthesizing carbohydrates have revealed the enormous complexity of the glycome,[1,2] which is more diverse than both the genome and proteome. However, the glycome alone does not offer insight into the biological functions of carbohydrates. In order to understand and exploit biological glycan functions, glycan behaviors have to be analyzed in detail both biochemically and microbiologically. Central to the emerging field of functional glycomics must be the development of technologies to identify specific carbohydrate binding partners. Carbohydrates are predominantly on the cell surface of organisms and occur as glycoconjugates in the form of glycoproteins, proteoglycans, and glycolipids.[3] Such cell surface glycans regulate interactions of the cell with the extracellular environment. Carbohydrate–protein interactions, in particular, are known to be crucial to most mammalian physiological processes as mediators of cell adhesion and signal transduction, and organizers of protein interactions.[4–6]

Furthermore, for eukaryotes, prokaryotes, and viruses, glycans hold tremendous, yet currently underexplored, potential as both diagnostic and therapeutic targets.[7,8] In fact, the surfaces of bacteria, viruses, and parasites are also decorated with carbohydrates, several of which are recognized by the immune system. Interestingly, specific glycans have been localized on the surface of many infectious agents and also cancer cells. While the functions of many of those glycans are as yet unknown, it is notable that many are unique, a fact that hints at the possibility of undiscovered biological properties. In addition, these unusual glycans show promise as a safe, fast, and reliable means to screen for the presence of cancer cells and pathogens.[9]

Pioneering glycobiologists have produced sophisticated technologies to efficiently measure carbohydrate–protein interactions, such as glycan microarrays.[10–14] Here, we report the development of a simple system: a carbohydrate-based cantilever microarray biosensor. This novel tool provides new opportunities for investigating protein–carbohydrate interactions.

Using immobilized receptor molecules, such as nucleic acids, proteins, and lipids, as well as cells and microorganisms, cantilever arrays have been applied to a variety of problems to detect molecular interactions.[15–30] Cantilever microarray biosensors are robust and reliably detect intermolecular binding events in solution and in

* Address correspondence to peter.seeberger@mpikg.mpg.de, b.hermann@cens.de.

Received for review December 30, 2010 and accepted March 9, 2011.

**Published online March 09, 2011**
**10.1021/nn103626q**

air. Furthermore, cantilever arrays are extremely sensitive and can detect picomolar amounts of mRNA in a complex background.[15] The principle behind the cantilever sensing mechanism is the transduction of biomolecular interactions into a nanomechanical force. Analyte binds to receptor molecules that are immobilized on the surface of the cantilever, and this causes changes in surface stress due to steric and/or electrostatic repulsion or attraction. This, in turn, generates a nanomechanical force that bends the cantilever. An optical laser, focused on the cantilever apex, is deflected as the cantilever bends, allowing for direct measurement of receptor−analyte binding. Cantilever arrays have advantages over other sensor techniques, including the ability to measure binding interactions in real time, and the capacity for multiple binding events to be examined simultaneously in up to eight parallel channels. In addition, the display of carbohydrates on the cantilever surface mimics the presentation of carbohydrates on the cell surface and allows for multivalent binding interactions that strengthen the often weak individual carbohydrate binding event. A unique cantilever feature is that, with a modified setup, measurements can be conducted in air as well as in solution, which may be particularly useful for detecting microbes. Furthermore, in contrast to most comparable technologies, small amounts of receptor and analyte are needed, and molecular labels are not required.

The carbohydrate-based cantilever sensor reported here was developed to detect biologically important carbohydrate−protein interactions. To test our system, we examined the clinically significant interaction between the antiviral protein cyanovirin-N (CV-N) and oligomannosides. CV-N is an 11 kDa protein isolated from cyanobacteria and has been shown to recognize mannosides on gp120, the heavily glycosylated envelope protein of the human immunodeficiency virus (HIV).[31,32] CV-N has been shown to have potent antiviral activity and works by irreversibly attaching to the nonamannose arms decorating gp120 and preventing the conformational changes necessary for HIV−cell fusion.[33] To measure the CV-N−oligomannoside binding interaction in real time, we created cantilevers with an oligomannose-sensing layer poised to bind CV-N. Our results demonstrate that this cantilever biosensor can reliably recognize picomolar concentrations of CV-N, while the sensor signal can be used to discriminate between oligomannosides. The sugar specificity of binding was demonstrated by competition experiments where free carbohydrate molecules were present in the buffer solution. Our work exemplifies the utility of carbohydrate-based cantilever biosensors as a tool for screening clinically significant carbohydrate−protein interactions and paves the way toward adapting this system to explore the glycome and to detect pathogens.

## RESULTS AND DISCUSSION

The cantilever array was prepared as a series of individual cantilevers each functionalized with either immobilized trimannose, nonamannose, or galactose (Figures 1 and 2). The top surface of each cantilever was coated with gold to permit thiol-functionalized oligomannosides to self-assemble and form a carbohydrate-based sensing layer. Thiol-functionalized galactoside was incorporated on further cantilevers as a control. Since galactose closely resembles mannose structurally, these galactose-functionalized cantilevers served as a stringent internal control for nonspecific binding events including (a) CV-N adsorption to the cantilever surface (front and backside), (b) nonspecific CV-N adsorption to galactose or the linker, and (c) a small number of binding events resulting from low-affinity binding to galactose *via* the CV-N binding pocket.

To guarantee comparable conditions among the sensing and control cantilevers, pairs of cantilevers within each array were functionalized with either trimannose or galactose under identical conditions. Each pair was incubated with the specific oligosaccharide for different times to optimize the carbohydrate densities on the surface in order to maximize the possible detection signals. The upper range of incubation times resulted in a more dense coating, whereas short incubation times produced more sparsely coated sensing layers (Figure 2).

Identifying the range of carbohydrate densities that generated the largest signal in response to the specific interaction between CV-N and oligomannose (the optimal binding density) is a crucial step in developing a high-quality sensor. In this study, for CV-N, optimal binding density was observed with cantilevers that were incubated from 9 to 15 min during functionalization. The strong binding affinity of CV-N for the trimannose-functionalized cantilevers used in this study indicates that CV-N has optimal access to the carbohydrates on these cantilever surfaces.

A significant advantage of cantilever biosensors over other techniques is that binding can be measured in real time. Time-dependent signal development patterns for CV-N−oligomannose binding were observed and are shown in Figure 3. After a period of system equilibration, where buffer was pumped through the measurement cell at a constant flow rate, CV-N was introduced into the measurement cell at a concentration of 0.1 mg/mL (9.1 $\mu$M) (shaded area, Figure 3). Specific and nonspecific CV-N binding induced initially tensile, and overall, mostly compressive, surface stresses that were relieved by the cantilever in turn bending upward (positive) or downward (negative).

The response to CV-N is plotted as both *averaged* and *differential* deflection signals. The *averaged* signal

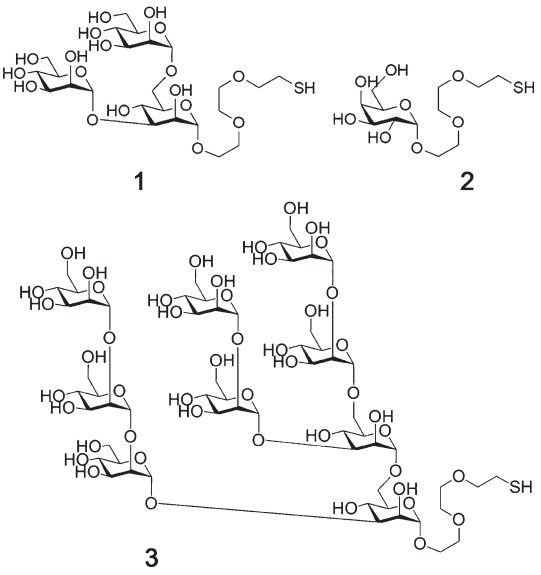


**Figure 1. Carbohydrate structures: Self-assembled monolayers of trimannoside (1), galactoside (2), and nonamannoside (3) that form the cantilever sensing layer for the detection of specific and nonspecific CV-N binding.**

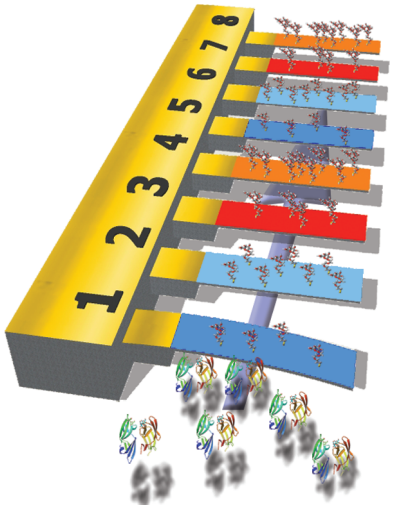


**Figure 2. Scheme of a cantilever array functionalized with thiol-terminated carbohydrates: While cantilevers 3, 4, 7, and 8 are coated with trimannose to detect CV-N, cantilevers 1, 2, 5, and 6 are coated with galactose as reference. Carbohydrate densities were adjusted using two different incubation times (1, 3, 5, 7 sparse and 2, 4, 6, 8 dense). Upon contact between the sensor surface and CV-N, protein binding will result in intermolecular interactions that induce surface stress on the cantilever surface that in turn is relieved by cantilever bending.**

represents the combined (*averaged*) measurements for each pair of identically functionalized cantilevers within an array (Figure 3, upper panel). Both *averaged* signals for CV-N binding to sparse or dense trimannose (orange/red) and nonspecific *averaged* deflection signals for CV-N binding to sparse or dense galactose (light/dark blue) were determined (Figure 3, upper panel). The *differential* signal represents specific recognition events between CV-N and trimannose and is

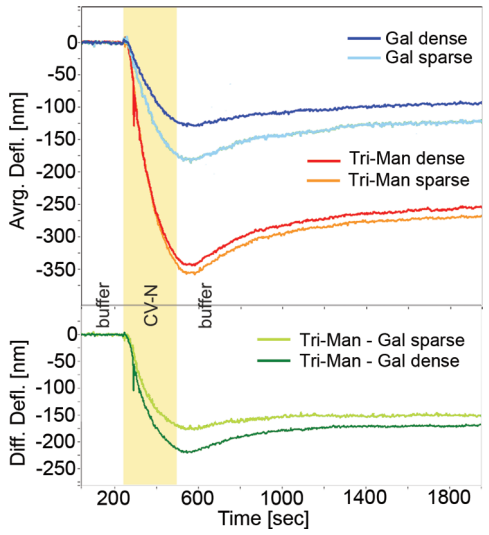


**Figure 3. *Averaged*/*differential* cantilever deflection as a function of time during CV-N detection (0.1 mg/mL (9.09 $\mu$M), shaded area). Top: Upon injection of CV-N, trimannose cantilevers (red and orange) show an about 3−4 times larger deflection signal than the galactose cantilevers (dark and light blue). The more sparsely functionalized trimannose layer (9 min, orange) shows a somewhat larger deflection than the more densely functionalized layer (14 min, red). Each graph represents an *average* signal of two identically functionalized cantilevers. Bottom: Corresponding *differential* signals for two different incubation times (9 min, light green and 14 min, dark green), calculated by subtracting the nonspecific galactose signals from the specific trimannose signals. The *differential* signal is assumed to reflect specific binding events. At the return of the running buffer, the differential signal recovers more slowly than the averaged signal, indicating dissociation of nonspecific binding.**

calculated by subtracting the *averaged* nonspecific signal (as determined by binding to the respective galactose-functionalized cantilevers) from the *averaged* signal of the mannose-functionalized cantilevers (Figure 3, lower panel). When calculating the *differential* signal, cantilevers with the same carbohydrate density, dense or sparse (red/dark blue and orange/light blue), were compared.

Both the more densely coated cantilevers (dark green, Figure 3) and the sparsely coated cantilevers (light green, Figure 3) produced strong *differential* signals upon exposure to CV-N. The *differential* pattern has notable differences from the *averaged* signal, which can be explained by the influences of specific and nonspecific molecular interactions on the cantilever surface.

Initially, the *averaged* signal exhibited a barely noticeable transient positive deflection for all cantilevers (Figure 3, upper panel). This effect is caused by nonspecific interactions and adsorption of CV-N since it is not evident in the *differential* signal (Figure 3, bottom panel). It is likely that the CV-N proteins tend to cluster on the cantilever surface due to hydrophobic interactions causing tensile surface stress and a small positive cantilever deflection (as reported for BSA elsewhere[34]).

The strong negative *averaged* and *differential* deflection observed approximately 50 s after CV-N arrival (Figure 3, both panels) is attributed to the effects of both specific and nonspecific CV-N adsorption. The strong negative deflection signals observed for the trimannose-functionalized cantilevers (orange/red, Figure 3), which are 3−4 times larger than that of galactose-functionalized cantilevers (light blue/dark blue, Figure 3), are a consequence of the higher binding affinity of CV-N for mannose. Compressive surface stress is generated by a combination of various processes taking place at the cantilever surface; electrostatic and hydrophobic protein−protein interactions due to charged protein side groups, as well as protein−surface interactions, may play key roles, as previously reported for IgG adsorption on gold-coated cantilever arrays.[34] For sparsely coated cantilevers, nonspecific binding interactions are predominantly contributing to a greater proportion of cantilever deflection and resulting in stronger *averaged* signals for these cantilevers. Although the cantilever signal quickly plateaus after protein injection when the buffer flow is stopped, inferring binding equilibrium, under experimental conditions the signal curve for each sample injection does not level due to the continuous pull of the buffer flow.

When comparing the *averaged* and *differential* signals for all cantilevers (Figure 3, top and bottom), a striking difference in the signal pattern is apparent at the end of the CV-N flow, when the buffer flow resumes. At this time, the *averaged* signal shows a strong movement in a positive direction (Figure 3, top panel, red/orange), suggesting removal of specifically and nonspecifically bound protein from the cantilever. A much weaker upward deflection is observed in the *differential* signal (Figure 3 bottom panel, green), indicating that specific binding is less affected by the change to buffer alone. Throughout the period of buffer flow, the *differential* signals continue to move upward very slowly, indicating that CV-N has a very low dissociation rate, presumably as a consequence of high CV-N avidity for immobilized, multivalent trimannose, rendering this interaction almost irreversible.[33] Thus, we did not extend the period of buffer flow beyond the standard washing time of 15 to 30 min between consecutive injections to observe whether the cantilevers completely return to the base levels observed prior to protein injection.

Cantilever sensing layers are formed using alkane thiol-modified carbohydrates that self-assemble on gold.[35,36] Experiments using octane thiol can indicate accessible gold surfaces remaining on a carbohydrate-functionalized cantilever, highlighting areas where CV-N and other proteins could potentially adsorb. Octane thiol blocking was employed to study the densities of trimannose, nonamannose, and galactose sensing layers since octane thiol would bind to the free

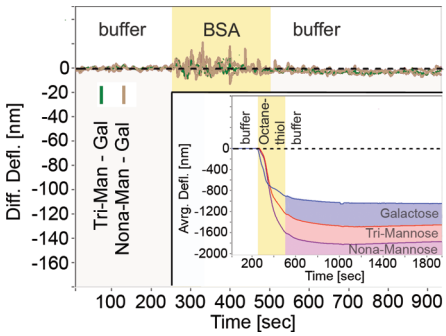


**Figure 4. Differential deflection as a function of time upon introduction of nonspecifically bound bovine serum albumin (BSA) after a series of CV-N measurements. The sensor shows no specific response to BSA. Inset: A surface density analysis of a freshly prepared cantilever (four nonamannose, two trimannose, and two galactose cantilevers) with an injection of an octanethiol block (0.1 mM). With increasing carbohydrate complexity more surface area becomes available to the small block molecules. However, CV-N self-blocking effectively quenches the available unspecific binding sites. This leads to a highly specific differential sensor signal shown by the nonspecific response to BSA.**

gold surfaces (see inset of Figure 4). Figure 4 shows that as the carbohydrate size and complexity increase, more free space is available on the cantilever surface for octane thiol adsorption, presumably due to the increased size of the headgroup. Nonspecific binding events were also examined with BSA (bovine serum albumin), a protein that does not bind either carbohydrate (see Figure 4) and therefore should not bind to the cantilever in a specific manner. The deflection of trimannose-, nonamannose-, and galactose-functionalized cantilevers in response to BSA was tested. After successful CV-N-detection experiments with these functionalized cantilevers, alternating injections of CV-N and BSA in equivalent concentrations were conducted. In case BSA ($6.31 \times 10^{-2}$ mg/mL (0.95 $\mu$M)) was introduced into the buffer flow (Figure 4), the averaged and differential response of the trimannose and nonamannose cantilevers to BSA was noisy, indicating that only nonspecific and transient binding interactions occurred. BSA has little effect on cantilever behavior after exposure to CV-N (Figure 4), because any free space available for nonspecific binding has been effectively blocked by nonspecifically adsorbed CV-N. These experiments prove that any differences in cantilever surface coverage that arise due to the self-assembly process and the distinct physical properties of the various carbohydrates are counterbalanced effectively by CV-N self-blocking. Since CV-N self-blocking does not affect specific binding and can be eliminated from the signal by calculating and considering the differential signal, we concluded that no additional steps were required to mitigate nonspecific binding.

Since cantilever bending is produced by molecular binding events on the cantilever surface, the magnitude of deflection is indicative of the strength and specificity of the carbohydrate−protein binding

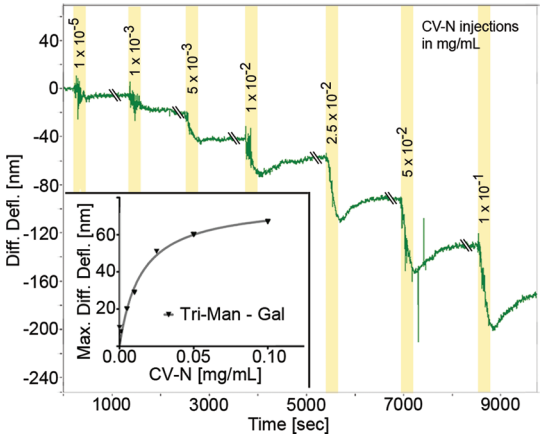


**Figure 5. Differential deflection as a function of time for sequential injections with increasing concentrations of CV-N (shaded areas). Only the running buffer returns between injections. The differential cantilever deflection increases with increasing CV-N concentrations, indicating a higher number of specific binding events. Inset: The maximum differential deflection is plotted with the concentration, and a Langmuir isotherm analysis is performed to determine the dissociation constant; see text.**

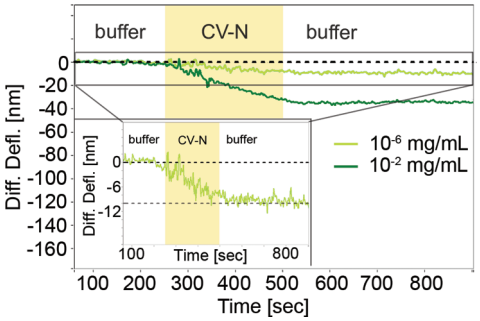


**Figure 6. The signal illustrates the sensitivity of the carbohydrate sensor with two consecutive CV-N injections plotted on top of each other for better comparison: After a CV-N injection at high concentration ($10^{-2}$ mg/mL (0.9 $\mu$M), dark green), the sensor is able to detect picomolar concentrations of CV-N ($10^{-6}$ mg/mL (90.9 pM), light green curve). The inset displays the differential deflection of picomolar injection on an enlarged *y*-axis indicating a low signal noise.**

interaction. To examine the effect of CV-N concentration on our system, a series of consecutive injections of increasing concentration of CV-N was conducted. Figure 4 shows the *differential* signal in response to seven such injections. Each injection took place without intermediate cleaning steps, except for the return of the running buffer. The trimannose cantilever array sensor reproducibly and systematically detects higher CV-N concentrations *via* larger *differential* deflection signals, exhibiting concentration-dependent deflection (Figure 5). Testing six independent cantilever arrays showed that 86% of compared injections were reproducible in their signal size within a standard deviation of 30%. The accuracy of the new sensor will improve as more experience with the system is gained. The concentration dependence is explained by the increased number of specific oligomannose−CV-N binding events that occur with increasing protein concentration.

Since the degree of *averaged* and *differential* cantilever deflection continues to increase, even at high protein concentrations, we can assume that the sensor is operated far from the maximum binding concentration. Even when tested with very high concentrations of CV-N (0.1 mg/mL) pumped at the lowest speed (0.42 $\mu$L/s), the sensor signal increases. This finding infers the robustness of the system and indicates that CV-N−oligomannose binding is a process with comparable on and off rates. Furthermore, the sensor is a physically robust tool that can be dried, stored at −20 °C, and reused many times with comparable performance.

In order to determine CV-N−oligomannose binding quantitatively, the maximum *differential* deflection signals were plotted as a function of protein concentrations (inset, Figure 5). From these data, assuming that individual carbohydrate−protein binding events on the cantilever surface are independent and unaffected by neighboring binding events (1:1 binding model), the dissociation constant ($K_d$) was determined by Langmuir isotherm analysis. The Langmuir isotherm states

$$\text{maximum differential deflection} = a \times c/(K_d + c)$$

where $c$ is the concentration and $a$ is a proportionality constant. Several series of measurements of protein concentration versus binding yielded an average $K_d$ value of 1.06 ± 0.69 $\mu$M for the CV-N−trimannose complex. The obtained $K_d$ value agrees with a published $K_d$ value for CV-N binding to a comparable dimannoside that has been measured as 1.5 $\mu$M.[37]

A biosensor must be able to detect nanomolar concentrations of analyte in order to be useful for clinically relevant analyses. Accordingly, we assessed the capacity for the carbohydrate cantilever sensor to detect CV-N at a low level under challenging circumstances. Very low concentrations of CV-N of $10^{-6}$ mg/mL (91 pM) were injected into the measurement cell directly after very high concentrations of $10^{-2}$ mg/mL (0.9 $\mu$M) (Figure 6). Indeed, protein concentrations as low as $10^{-6}$ mg/mL (91 pM) could be detected even immediately following injections with high concentrations of protein. Generally, the magnitude of a cantilever response to a protein is indicative of the strength of the binding interaction. We observed it to be reproducible and not influenced by any previous injection, no matter whether the previous injection was with a higher or lower concentration of protein. Furthermore, time-consuming cleaning steps are not required between injections. Due to these features, this system fares well in comparison to other cantilever-based array protein detection assays that do not rely on carbohydrate−protein interactions, but

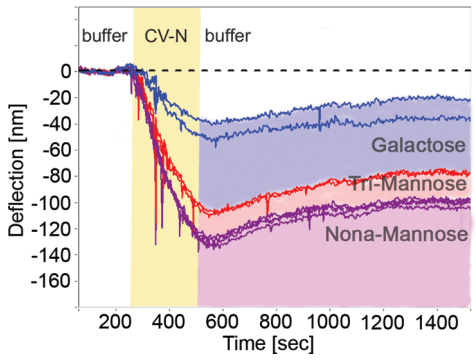


**Figure 7. Time evolution of deflection of four nonamannoside-, two trimannoside-, and two galactoside-functionalized cantilevers upon CV-N injection (0.1 mg/mL (9.1 $\mu$M)). The nonamannoside deflection is roughly 20% stronger than for trimannose. Hence, the sensor can successfully discriminate between the two oligomannosides.**

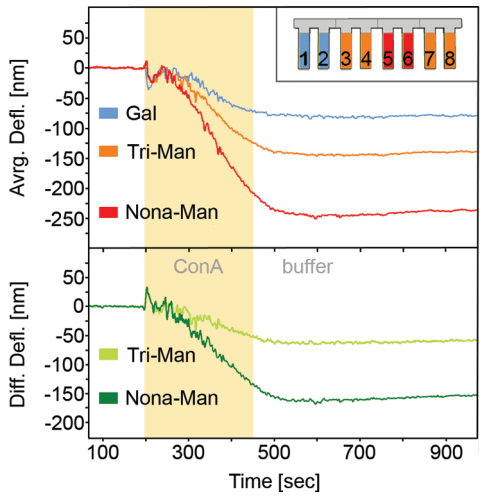


**Figure 8. Average and differential ConA binding signals. Upper panel: Following injection of ConA (2 mg/mL; 19.2 $\mu$M) the average deflection of tri- and nonamannose-coated cantilevers was considerably larger than the average deflection of the galactose reference cantilevers. Multivalent and multisite binding by nonamannose resulted in increased deflection. The inset illustrates cantilever array functionalization. Lower panel: The differential deflections represent the specific binding of Con-A to trimannose and nonamannose cantilevers after correction for the nonspecific binding using the galactose reference cantilever.**

antigen−antibody[26−28] or antigen−antibody-sandwich assays.[29] Most importantly, our detection sensitivity (91 pM) compares well to the best reported sensitivities that range in the lower nanomolar regime.[27,28,38]

To further analyze the sensitivity of our system, we investigated whether the magnitude of the cantilever response to CV-N binding varied in accordance with the particular oligomannoside that made up the sensing layer. If so, our carbohydrate sensor could distinguish between CV-N binding to galactose, trimannose, and nonamannose. To this end, three sets of cantilevers were prepared with galactose, trimannose, or nonamannose cantilever sensor layers, each with the same oligosaccharide concentration. Figure 7 shows the deflection signal of four nonamannose-, two trimannose-, and two galactose-functionalized cantilevers. The degree of cantilever deflection correlates with the amount of bound protein, which is dependent on the protein concentration (discussed earlier), the binding strength of the analyte (possibly influenced by the position of the carbohydrate on the surface), and the coupled carbohydrate (binding partner): the nonamannose-functionalized cantilevers exhibit a 20% stronger deflection than trimannose-functionalized cantilevers, underlining the stronger affinity of CV-N for nonamannose due to its known multivalent and multisite binding.[33]

To validate the general utility of the sensor, a second carbohydrate binding protein was analyzed. ConcanavalinA (ConA) is a tetrameric protein consisting of four identical subunits each bearing one high-affinity mannose binding site.[39] Several cantilever arrays were functionalized with trimannose and nonamannose as sensor layers as well as with galactose as reference. *Averaged* and *differential* deflection signals following ConA injections (2 mg/mL (19.2 $\mu$M)) are depicted in Figure 8. During a typical injection of a ConA sample, negative deflection for all carbohydrate-coated cantilevers was observed. The *averaged* and *differential* response of the tri- and nonamannose-functionalized cantilevers was significantly stronger than the responses of cantilevers covered with galactose. Indeed, the deflection of nonamannoside-coated cantilevers was significantly larger than that for trimannosides.

Proteins, bound to the anchored carbohydrate, interact with the cantilever surface due to steric and electrostatic forces between charged protein side groups. The resulting compressive surface stress leads in turn to the observed cantilever bending. Nonamannose is more likely to bind ConA in a multivalent fashion than trimannose, and the observed differences in signal size are attributed to these effects. Deflection of the galactose reference cantilevers is attributed to nonspecific binding to galactose, the thiol linker, and the cantilever surface.

In addition to the *averaged* signals, the *differential* deflection was calculated as before, by subtracting the galactose signals from the mannose signals. The resulting graphs represent the specific binding of the ConA analyte to the sensor. Accordingly, the *differential* deflection for the specific nonamannose signal is larger than that of the specific trimannose signal (Figure 8, lower panel).

As for CV-N, the concentration dependence, sensitivity, and specificity of our sensor for ConA binding was tested. Again, the sensor signal increases with increasing protein concentrations. The Langmuir isotherm analysis yielded a $K_d$ value of 15.3 $\mu$M, which

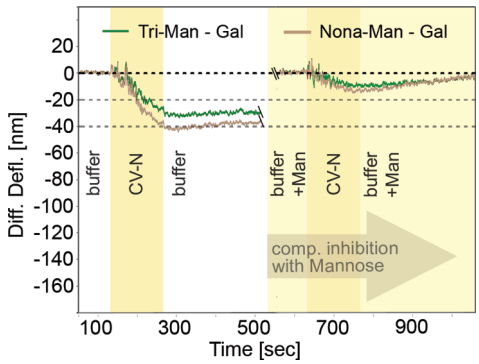


**Figure 9. Differential deflection of a cantilever without and in the presence of mannose in the running buffer demonstrating the selectivity of the sensor setup. Injection of 0.1 mg/mL (9.1 $\mu$M) CV-N leads to cantilever bending of 30 and 40 nm for trimannose and nonamannose cantilevers, respectively. When free mannose (100 mM) is added to CV-N (0.1 mg/mL (9.1 $\mu$M)), reduced cantilever bending (10 and 15 nm, respectively) is observed. The mannose molecules block CV-N binding pockets and compete with the mannoside immobilized on the cantilever surface. The reduced signal upon competitive inhibition confirms the high selectivity of CV-N detection.**

compares well to the literature.[40] Nanomolar concentrations of ConA (1 $\mu$g/mL (9.6 nM)) can be detected even when immediately following a highly concentrated injection of ConA (10 mg/mL (96.2 $\mu$M)). This sensitivity compares well to standard surface-bound techniques such as surface plasmon resonance (SPR), quartz crystal microbalance (QCM), and glycan microarrays.[41] To approximate more realistic, complex solutions, we finally conducted measurements in the presence of background BSA (0.007 mg/mL; 0.1 $\mu$M). At ConA sample concentrations of 2 mg/mL (19.2 $\mu$M) signal sizes of 55 nm compare well to the signals without BSA (Figure 8). These results underscore the selectivity of protein binding to the carbohydrates on the cantilever array sensor.

Competitive inhibition assays demonstrate the highly selective nature of the sensor. Free mannose was added to the running buffer to compete with bound immobilized oligomannose for CV-N. Figure 9 shows that the size of the *differential* signal strongly decreases (by about two-thirds on average) in the presence of free mannose in solution. Inhibition of specific oligomannose–CV-N binding on the cantilever surface is the result of CV-N binding to mannose in solution with regard to the respective binding strength of carbohydrates in solution and surface-bound carbohydrates. CV-N is therefore unavailable to bind the cantilever sensor. The reduced incidence of binding events on the cantilever surface decreases the degree of cantilever deflection. Competitive inhibition independently confirms both the effectiveness and selectivity of the cantilever array design and the high affinity of CV-N and ConA for mannosides anchored on the sensor surface.

## CONCLUSION

We describe the development of a cantilever array biosensor that is designed to detect clinically relevant carbohydrate–protein interactions. This sensor can detect picomolar amounts of CV-N, an oligomannoside-binding protein. Indeed, picomolar sensitivity was achieved even after injections of high protein concentrations. The sensor is reliable, sensitive, selective, readily prepared, and reusable. Our cantilever array biosensor represents the first carbohydrate–protein detection tool in the rapidly expanding field of glycomics that was developed using the interaction of the antiviral protein cyanovirin-N and oligomannosides as example. Further development of this assay will lead to quick, sensitive methods to study other, medically relevant carbohydrate–protein interactions.

## MATERIALS AND METHODS

**Analyte/Buffers.** Thiol-terminated carbohydrate (nonamannose, trimannose, and galactose) derivates were synthesized as described elsewhere.[42] Cynanovirin-N was purified as described elsewhere.[31] ConA was purchased from Sigma. A running buffer consisting of a solution of 10 mM Tris, pH 7.7, 100 mM NaCl, 1 mM $CaCl_2$, and 0.005% Tween-20 was prepared.

**Cantilever Sensor Surface Functionalization.** Arrays consisting of eight identical silicon cantilevers (500 $\mu$m × 100 $\mu$m × 1 $\mu$m) on a support were coated on the top side with a 20 nm layer of gold (Concentris GmbH, Switzerland). All cantilever arrays were washed in ultrapure water and ethanol followed by a UV-ozone cleaning cycle immediately prior to functionalization. Individual cantilevers were functionalized in parallel by inserting them for a time between 7 and 25 min into an array of liquid-filled microcapillaries inside the functionalization unit (Concentris GmbH, Switzerland). The functionalization solution contained the respective carbohydrate derivate at a concentration of 40 $\mu$M in 10 mM Tris buffer, pH 7.7.

**Instrument.** The commercial Cantisens sensor platform (Concentris GmbH, Switzerland) contains a measurement cell of 5 $\mu$L and is operated by an automated liquid handling system. The integrated temperature control with extra preheating stage for the injected sample offers a stability of 0.01 °C. The cantilever array is mounted, *via* a sensor cartridge, inside the measurement cell and kept under a continuous flow of running buffer. For measurements, 100 $\mu$L of the sample solution is injected into a sample loop and plugged into the buffer flow reaching the measurement chamber at the desired time. The resulting nanomechanical deflection of each cantilever is detected in real time by sampling the deflection of a laser beam emitted from an array of eight parallel VCSELs (vertical cavity surface emitting lasers). LabView-based software allows for instrument control and signal processing. The signal curves of all cantilevers were corrected for constant drift. Where indicated, the signals of identically functionalized cantilevers were *averaged*; *differential* signals were calculated by subtracting the unspecific reference signal from the specific recognition signal. The Langmuir adsorption analysis was performed with GraphPad Prism version 5.03 for Windows, GraphPad Software, San Diego, CA, USA, www.graphpad.com, using a minimal model that includes one site-specific binding and assumes that the concentration of bound protein is negligible in comparison to the total protein

concentration. Therefore concentration of nonbound protein equals the concentration of the injected protein concentration (cCV-N bound = cCV-N total) in our model.

**Heat Test.** Exposing cantilever arrays to a slight temperature change is an ideal test for determining quality variations of the individual cantilevers due to the fabrication and/or coating. A change of the temperature (*e.g.*, from 22 to 25 °C) in the measurement chamber results in a deflection of each cantilever that is caused by the bimetallic makeup of the silicon cantilevers with their respective gold coating, reflecting possible differences of the mechanical response. Due to the larger coefficient of thermal expansion of the gold coating on top of the silicon cantilevers, all cantilevers should bend downward when the temperature rises and bend upward when the temperature drops. Thus, when all cantilevers behave in a comparable way, artifacts caused by fabrication or functionalization procedures can be excluded. Only cantilever arrays that displayed comparable deflections of the individual cantilevers in a heat test were employed.

**Carbohydrate−Protein Detection Experiments.** After mounting an array inside the measurement cell, a constant buffer flow of 0.42 $\mu$L/s and a constant temperature of 22 °C were established. The array was equilibrated under these conditions for several hours until a constant drift was achieved.[16] CV-N and ConA samples were taken up in running buffer and centrifuged prior to injection.

*Acknowledgment.* We acknowledge the ERA-Chemistry program, NRP47, NCCR−Nanoscale Science, Center for Nano Science (CeNS), and the excellence cluster Nanosystems Initiative Munich (NIM), the elite network of Bavaria and the Walther-Meissner-Institute, Bavarian Academy of Science and Humanities, for financial support. We thank the ETH Zurich, the Swiss National Fonds (SNF), and the Max-Planck-Society for generous financial support. We thank B. O'Keefe for generously providing the CV-N samples. We are thankful for equipment cooperation with the groups of Prof. M.-C. Amann (Walter-Schottky-Institute), Prof. J. Kotthaus, Prof. J. Rädler (both LMU Munich), and Concentris GmbH. Scientific discussions with and support by J. Köser, U. Hubler, M. Bammerlin, F. Trixler, M. Hennemeyer, R. Stark, T. Sobey, D. Heinrich, V. Schittler, S. Nieratschker, S. Jannuzzi, J. Büttner, C. Rohr, and A. Malecki are gratefully acknowledged. We thank C. Rohr for help with the artwork. Technical support of A. Habel, K. Helm-Knapp, J. Geismann, and H. Thies and co-workers is gratefully appreciated. We thank Dr. V. Mountain for critically editing the manuscript.

*Supporting Information Available:* Details on ConA recognition concerning specificity, sensitivity, and concentration dependence on this carbohydrate-based cantilever sensor. Nonspecific binding on cantilever arrays before exposure to lectins tested with BSA. This material is available free of charge *via* the Internet at http://pubs.acs.org.

## REFERENCES AND NOTES

1. Bertozzi, C. R.; Kiessling, L. L. Chemical Glycobiology. *Science* **2001,** *291*, 2357–2364.
2. Plante, O. J.; Palmacci, E. R.; Seeberger, P. H. Automated Solid-Phase Synthesis of Oligosaccharides. *Science* **2001,** *291*, 1523–1527.
3. Varki, A.; Cummings, R. D.; Esko, J. D.; Freeze, H. H.; Stanley, P.; Bertozzi, C. R.; Hart, G. W.; Etzler, M. E.; Akimoto, Y.; Brockhausen, I.; *et al*. In *Essentials of Glycobiology*, 2nd ed.; Varki, A.; Cummings, R. D.; Esko, J. D.; Freeze, H. H.; Stanley, P.; Bertozzi, C. R.; Hart, G. W.; Etzler, M. E., Eds.; Cold Spring Harbor Laboratory Press: Woodbury, NY, 2009.
4. Lowe, J. B. Glycosylation, Immunity and Autoimmunity. *Cell* **2001,** *104*, 809–812.
5. Kansas, G. S. Selectins and their Ligands: Current Concepts and Controversies. *Blood* **1996,** *88*, 3259–3287.
6. Danishefsky, S. J.; Allen, J. R. From the Laboratory to the Clinic: A Retrospective on Fully Synthetic Carbohydrate-Based Anticancer Vaccines. *Angew. Chem., Int. Ed.* **2000,** *39*, 836–863.
7. Seeberger, P. H.; Werz, D. B. Automated Synthesis of Oligosaccharides as a Basis for Drug Discovery. *Nat. Rev. Drug. Discovery* **2005,** *4*, 751–763.
8. Seeberger, P. H.; Werz, D. B. Synthesis and Medical Applications of Oligosaccharides. *Nature* **2007,** *446*, 1046–1051.
9. Tamborrini, M.; Werz, D. B.; Frey, J.; Pluschke, G.; Seeberger, P. H. Anti-Carbohydrate Antibodies for the Detection of Anthrax Spores. *Angew. Chem., Int. Ed.* **2006,** *45*, 6581–6582.
10. Blixt, O.; Head, S.; Mondala, T.; Scanlan, C.; Huflejt, M. E.; Alvarez, R.; Bryan, M. C.; Fazio, F.; Calarese, D.; Stevens, J.; *et al*.Printed Covalent Glycan Array for Ligand Profiling of Diverse Glycan Binding Proteins. *Proc. Natl. Acad. Sci. U. S. A.* **2004,** *101*, 17033–17038.
11. Fukui, S.; Feizi, T.; Galustian, C.; Lawson, A. M.; Chai, W. Oligosaccharide Microarrays for High-Throughput Detection and Specificity Assignments of Carbohydrate-Protein Interactions. *Nat. Biotechnol.* **2002,** *20*, 1011–1017.
12. Ratner, D. M.; Adams, E. W.; Disney, M. D.; Seeberger, P. H. Tools for Glycomics: Mapping Interactions of Carbohydrates in Biological Systems. *Chembiochem* **2004,** *5*, 1375–1383.
13. Paulson, J. C.; Blixt, O.; Collins, B. E. Sweet Spots in Functional Glycomics. *Nat. Chem. Biol.* **2006,** *2*, 238–248.
14. Horlacher, T.; Seeberger, P. H. Carbohydrate Arrays as Tools for Research and Diagnostics. *Chem. Soc. Rev.* **2008,** *37*, 1414–1422.
15. Zhang, J.; Lang, H. P.; Huber, F.; Bietsch, A.; Grange, W.; Certa, U.; McKendry, R.; Güntherodt, H.-J.; Hegner, M.; Gerber, Ch. Rapid and Label-Free Nanomechanical Detection of Biomarker Transcripts in Human RNA. *Nat. Nanotechnol.* **2006,** *1*, 214–220.
16. McKendry, R.; Zhang, J.; Arntz, Y.; Strunz, T.; Hegner, M.; Lang, H. P.; Baller, M. K.; Certa, U.; Meyer, E.; Güntherodt, H.-J.; Gerber, Ch. Multiple Label-Free Biodetection and Quantitative DNA-Binding Assays on a Nanomechanical Cantilever Array. *Proc. Natl. Acad. Sci. U. S. A.* **2002,** *99*, 9783–9788.
17. Fritz, J.; Baller, M. K.; Lang, H. P.; Rothuizen, H.; Vettiger, P.; Meyer, E.; Güntherodt, H.-J.; Gerber, Ch.; Gimzewski, J. K. Translating Biomolecular Recognition into Nanomechanics. *Science* **2000,** *288*, 316–318.
18. Hansen, K. M.; Ji, H.-F.; Wu, G.; Datar, R.; Cote, R.; Majumdar, A.; Thundat, T. Cantilever-Based Optical Deflection Assay for Discrimination of DNA Single-Nucleotide Mismatches. *Anal. Chem.* **2001,** *73*, 1567–1571.
19. Park, J.; Ryu, J.; Choi, S. K.; Seo, E.; Cha, J. M.; Ryu, S.; Kim, J.; Kim, B.; Lee, S. H. Real-Time Measurement of the Contractile Forces of Self-Organized Cardiomyocytes on Hybrid Biopolymer Microcantilevers. *Anal. Chem.* **2005,** *77*, 6571–6580.
20. Gfeller, K. Y.; Nugaeva, N.; Hegner, M. Micromechanical Oscillators as Rapid Biosensor for the Detection of Active Growth of *Escherichia coli*. *Biosens. Bioelectron.* **2005,** *21*, 528–533.
21. Gfeller, K. Y.; Nugaeva, N.; Hegner, M. Rapid Biosensor for Detection of Antibiotic-Selective Growth of *Escherichia coli*. *Appl. Environ. Microbiol.* **2005,** *71*, 2626–2631.
22. Pera, I.; Fritz, J. Sensing Lipid Bilayer Formation and Expansion with a Microfabricated Cantilever Array. *Langmuir* **2007,** *23*, 1543–1547.
23. Huber, F.; Hegner, M.; Gerber, C.; Güntherordt, H. J.; Lang, H. P. Label Free Analysis of Transcription Factors Using Microcantilever Arrays. *Biosens. Bioelectron.* **2006,** *21*, 1599–1605.
24. Ndieyira, J. W.; Watari, M.; Barrera, A. D.; Zhou, D.; Vögtli, M.; Batchelor, M.; Cooper, M. A.; Strunz, T.; Horton, M. A.; Abell, Ch.; Rayment, T.; Aeppli, G.; McKendry, R. A. Nanomechanical Detection of Antibiotic-Mucopeptide Binding in a Model for Superbug Drug Resistance. *Nat. Nanotechnol.* **2008,** *3*, 691–696.
25. Braun, T.; Ghatkesar, M. K.; Backmann, N.; Grange, W.; Boulanger, P.; Letellier, L.; Lang, H.-P.; Bietsch, A.; Gerber, Ch.; Hegner, M. Quantitative Time-Resolved Measurement of Membrane Protein-Ligand Interactions Using Microcantilever Array Sensors. *Nat. Nanotechnol.* **2008,** *4*, 179–185.
26. Wu, G.; Datar, R. H.; Hansen, K. M.; Thundat, T.; Cote, R. J.; Majumdar, A. Bioassay of Prostate-Specific Antigen (PSA)

Using Microcantilevers. *Nat. Biotechnol.* **2001,** *19*, 856–860.
27. Yue, M.; Stachowiak, J. C.; Lin, H.; Datar, R.; Cote, R.; Majumdar, A. Label-Free Protein Recognition Two-Dimensional Array Using Nanomechanical Sensors. *Nano Lett.* **2008,** *8*, 520–524.
28. Backmann, N.; Zahnd, Ch.; Huber, F.; Bietsch, A.; Plückthun, A.; Lang, H.-P.; Güntherodt, H.-J.; Hegner, M.; Gerber, Ch. A Label-Free Immunosensor Array Using Single-Chain Antibody Fragments. *Proc. Natl. Acad. Sci. U. S. A.* **2005,** *102*, 14587–14592.
29. Lam, Y.; Abu-Lail, N. I.; Alam, M. S.; Zauscher, S. Using Microcantilever Deflection to Detect HIV-1 Envelope Glycoprotein gp120. *Nanomed. Nanotechnol. Biol. Med.* **2006,** *2*, 222–229.
30. Tzeng, T.-R. J.; Cheng, Y. R.; Saeidpourazar, R.; Aphale, S. S.; Jalili, N. Adhesin-Specific Nanomechanical Cantilever Biosensors for Detection of Microorganisms. *J. Heat Transfer* **2010,** *133*, 011012.
31. Boyd, M. R.; Gustafson, K. R.; McMahon, J. B.; Shoemaker, R. H.; O'Keefe, B. R.; Mori, T.; Gulakowski, R. J.; Wu, L.; Rivera, M. I.; Laurencot, C. M.; *et al*. Discovery of Cyanovirin-N, a Novel Human Immunodeficiency Virus-Inactivating Protein that Binds Viral Surface Envelope Glycolprotein gp120: Potential Applications to Microbicide Development. *Antimicrob. Agents Chemother.* **1997,** *41*, 1521–1530.
32. Bolmstedt, A. J.; O'Keefe, B. R.; Shenoy, S. R.; McMahon, J. B.; Boyd, M. R. Cyanovirin-N Defines a New Class of Antiviral Agent Targeting N-Linked, High-Mannose Glycans in an Oligosaccharide-Specific Manner. *Mol. Pharmacol.* **2001,** *59*, 949–954.
33. Shenoy, S. R.; Barrientos, L. G.; Ratner, D. M.; O'Keefe, B. R.; Seeberger, P. H.; Gronenborn, A. M.; Boyd, M. R. Multisite and Multivalent Binding between Cyanovirin-N and Branched Oligomannosides: Calorimetric and NMR Characterization. *Chem. Biol.* **2002,** *9*, 1109–1118.
34. Moulin, A. M.; O'Shea, S. J.; Badley, R. A.; Doyle, P.; Welland, M. E. Measuring Surface-Induced Conformational Changes in Proteins. *Langmuir* **1999,** *15*, 8776–8779.
35. Xu, S.; Cruchon-Dupeyrat, S. J. N.; Garno, J. C.; Liu, G.-Y.; Kane Jennings, G.; Yong, T.-H.; Laibinis, P. E. In Situ Studies of Thiol Self-Assembly on Gold from Solution Using Atomic Force Microscopy. *J. Chem. Phys.* **1998,** *108*, 5002–5012.
36. Godin, M.; Williams, P. J.; Tabard-Cossa, V.; Laroche, O.; Beaulieu, L. Y.; Lennox, R. B.; Grütter, P. Surface Stress, Kinetics, and Structure of Alkanethiol Self-Assembled Monolayers. *Langmuir* **2004,** *20*, 7090–7096.
37. Liang, P.-H.; Wang, S.-K.; Wong, C.-H. Quantitative Analysis of Carbohydrate-Protein Interactions Using Glycan Microarrays: Determination of Surface and Solution Dissociation Constants. *J. Am. Chem. Soc.* **2007,** *129*, 11177–11184.
38. Bewley, C. A.; Otero-Quintero, S. The Potent Anti-HIV Protein Cyanovirin-N Contains Two Novel Carbohydrate Binding Sites That Selectively Bind to $Man_8$ D1D3 and $Man_9$ with Nanomolar Affinity: Implications for Binding to the HIV Envelope Protein gp120. *J. Am. Chem. Soc.* **2001,** *123*, 3892–3902.
39. Wang, J. L.; Cunningham, B. A.; Edelman., G. M. Unusual Fragments in the Subunit Structure of Concanavalin A. *Proc. Natl. Acad. Sci. U. S. A.* **1971,** *68*, 1130–1134.
40. Zhang, Y.; Luo, S.; Tang, Y.; Yu, L.; Hou, K.-Y.; Cheng, J.-P.; Zeng, X.; Wang, P. G. Carbohydrate-Protein Interactions by "Clicked" Carbohydrate Self-Assembled Monolayers. *Anal. Chem.* **2006,** *78*, 2001–2008.
41. Park, S.; Lee, M.; Pyo, S.-J.; Shin, I. Carbohydrate Chips for Studying High-Throughput Carbohydrate-Protein Interactions. *J. Am. Chem. Soc.* **2004,** *126*, 4812–4819.
42. Ratner, D. M.; Plante, O. J.; Seeberger, P. H. A Linear Synthesis of Branched High-Mannose Oligosaccharides from the HIV-1 Viral Surface Envelope Glycoprotein gp120. *Eur. J. Org. Chem.* **2002,** 826–833.